



Contents lists available at ScienceDirect

Journal of Ginseng Research

journal homepage: <http://www.ginsengres.org>

Research Article

Ginsenoside Rb2 suppresses the glutamate-mediated oxidative stress and neuronal cell death in HT22 cells

Dong Hoi Kim^{1,☆}, Dae Won Kim^{2,☆}, Bo Hyun Jung^{3,☆}, Jong Hun Lee³, Heesu Lee³, Gwi Seo Hwang^{4,*}, Ki Sung Kang^{4,*}, Jae Wook Lee^{1,5,**}¹ Convergence Research Center for Dementia, KIST, Seoul, Republic of Korea² Department of Biochemistry, College of Dentistry, Gangneung Wonju National University, Gangneung, Republic of Korea³ Department of Oral Anatomy, College of Dentistry, Gangneung Wonju National University, Gangneung, Republic of Korea⁴ College of Korean Medicine, Gacheon University, Seongnam, Republic of Korea⁵ Natural Constituent Research Center, KIST, Gangneung, Republic of Korea

ARTICLE INFO

Article history:

Received 9 July 2018

Received in Revised form

21 October 2018

Accepted 7 December 2018

Available online 15 December 2018

Keywords:

Ginsenoside Rb2

Neurotoxicity

MAPK

Reactive oxygen species

ABSTRACT

Background: The objective of our study was to analyze the neuroprotective effects of ginsenoside derivatives Rb1, Rb2, Rc, Rd, Rg1, and Rg3 against glutamate-mediated neurotoxicity in HT22 hippocampal mouse neuron cells.

Methods: The neuroprotective effect of ginsenosides were evaluated by measuring cell viability. Protein expressions of mitogen-activated protein kinase (MAPK), Bcl2, Bax, and apoptosis-inducing factor (AIF) were determined by Western blot analysis. The occurrence of apoptotic and death cells was determined by flow cytometry. Cellular level of Ca²⁺ and reactive oxygen species (ROS) levels were evaluated by image analysis using the fluorescent probes Fluor-3 and 2',7'-dichlorodihydrofluorescein diacetate, respectively. *In vivo* efficacy of neuroprotection was evaluated using the Mongolian gerbil of ischemic brain injury model.

Result: Reduction of cell viability by glutamate (5 mM) was significantly suppressed by treatment with ginsenoside Rb2. Phosphorylation of MAPKs, Bax, and nuclear AIF was gradually increased by treatment with 5 mM of glutamate and decreased by co-treatment with Rb2. The occurrence of apoptotic cells was decreased by treatment with Rb2 (25.7 μM). Cellular Ca²⁺ and ROS levels were decreased in the presence of Rb2, and *in vivo* data indicated that Rb2 treatment (10 mg/kg) significantly diminished the number of degenerated neurons.

Conclusion: Our results suggest that Rb2 possesses neuroprotective properties that suppress glutamate-induced neurotoxicity. The molecular mechanism of Rb2 is by suppressing the MAPKs activity and AIF translocation.

© 2019 The Korean Society of Ginseng, Published by Elsevier Korea LLC. This is an open access article under the CC BY-NC-ND license (<http://creativecommons.org/licenses/by-nc-nd/4.0/>).

1. Introduction

Glutamate is the prime excitatory neurotransmitter associated with diverse physiological functions of the nervous system including neuronal development, plasticity, and motor functions as well as the cognitive functions of the brain [1]. Physiologically, when the glutamate concentration in the brain increases, it leads to neurotoxicity due to the upsurge of intracellular reactive oxygen species (ROS) [2–5]. The ROS production is primarily implicated in

neuronal cell death of many acute brain injury and chronic neurodegenerative diseases such as Alzheimer's [6], Parkinson's [7], and Huntington's diseases [8]. The ROS surge is mainly caused by the excess extracellular glutamate which impairs the cysteine/glutamate antiporter's ability to transport cysteine inside the cell, thus the intracellular antioxidant glutathione amount dwindles [9–12]. Also, the depletion of glutathione accelerate various downstream of signaling pathways that leads to neuronal cell death through abnormal Ca²⁺ uptake and lipoxygenase-dependent lipid

* Corresponding author. College of Korean Medicine, Gacheon University, Seongnam, Republic of Korea.

** Corresponding author. Convergence Research Center for Dementia, KIST, Seoul, Republic of Korea.

E-mail addresses: kkang@gachon.ac.kr (K.S. Kang), jwlee5@kist.re.kr (J.W. Lee).

☆ These authors are equally contributed in this work.

peroxidation [11,13]. The aberrant Ca^{2+} flow inside the cell activates the calpain enzyme that truncates the proapoptotic Bid to tBid which activates apoptotic protein Bax [14,15]. Further, the oxidative stress causes mitochondrial dysfunction, and it triggers the apoptosis-inducing factor (AIF) translocation to the nucleus which end up activating the caspase independent apoptotic pathway [16,17]. AIF is flavoprotein with NADH oxidase activity and localized in mitochondria membrane. AIF translocated from mitochondria to nucleus when apoptosis is induced [18,19].

The oxidative stress generation galvanize the molecular events downstream by triggering the phosphorylation of mitogen-activated protein kinases (MAPKs), the extracellular signal-regulated kinase (ERK), and c-Jun N-terminal kinase (JNK), and p38 [20]. MAPKs activation also associated with transcriptional induction of various apoptosis genes [21]. And recent studies have shown that neuronal injuries caused by different cytokines, inflammation, or heat shock inducers trigger the JNK and p38 signaling pathways, and also the ERK signaling is sensitive to oxidative stress-mediated neuronal death [22,23]. Therefore, suppression of the MAPKs activation by glutamate-induced oxidative stress represents an interesting strategy for the prevention and treatment of neurodegenerative diseases.

Ginsenosides are steroid-like saponins, the major active compounds of ginseng that are typically recovered from the Korean medicinal herb *Panax ginseng* roots. Ginsenosides are categorized into 20(S)-protopanaxadiols (Rb1, Rb2, Rc, Rd, and Rg3) and 20(S)-protopanaxatriols (Re and Rg1) based on their aglycone moieties [24–26]. Ginseng extracts reportedly possess abundant antioxidant potentials and exhibit significant neuroprotective effects under different neuropathological conditions. Among the ginsenosides, Rb1 [27,28], Rg1 [29], Rd [30], and Rg3 [31] are known for their neuroprotective effect in ischemic brain injury, acute ischemic stroke, and cerebral ischemia in rats [32]. However, there is no report about the potential neuroprotective properties of ginsenoside Rb2 and other ginsenosides in a cell-based assay. In this study, we have compared the neuroprotective effects of ginsenosides, Rb1, Rb2, Rc, Rd, Rg1, and Rg3 in a cell-based assay and examined activity of ginsenoside Rb2 against glutamate-induced neurotoxicity and its underlying mechanisms. Further we have assessed the *in vivo* efficacy of Rb2 in an animal model of ischemic brain injury.

2. Materials and methods

2.1. Chemicals and reagents

Ginsenosides were bought from a commercial source (Ambo Institute, Seoul, South Korea) and used without further purification. The purity of each ginsenosides is as follows: ginsenoside Rb1: 98.26%, ginsenoside Rb2: 99.33%, ginsenoside Rc: 99.00%, ginsenoside Rd: 99.39%, ginsenoside Rg1: 100%, and ginsenoside 20(S)-Rg3: 98.0%. An 3-(4,5-dimethylthiazol-2-yl)-2,5-diphenyltetrazolium bromide (MTT) reagent was obtained from Dail Lab Service Co. (Seoul, South Korea). 2',7'-dichlorodihydrofluorescein diacetate (H_2DCFDA) fluorescent probe used for ROS measurement was bought from ThermoFisher (Waltham, MA, USA). Fluo-3 Calcium indicator was purchased from ThermoFisher (Waltham, MA, USA).

2.2. Cells culture

HT22 mouse hippocampal neuronal cells were cultured to test the neuroprotective effects of ginsenosides against glutamate-mediated neuronal cell toxicity using previous procedure [33]. HT22 cells were bought from the Korean Cell Line Bank (Seoul, South Korea) and grown in Dulbecco's Modified Eagle's Medium

(DMEM) (Hyclone Co.) mixed with 10% fetal bovine serum (Gibco Co.), 1% penicillin/streptomycin, and 4 mM L-glutamine using an incubator with 5% CO_2 at 37 °C [33].

2.3. MTT assay

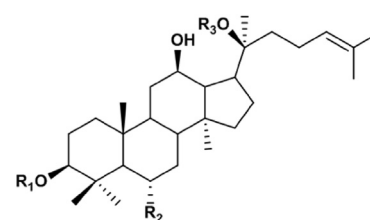
Cultured HT22 cells were added in 96-well plates at a density of 4×10^3 cells/well and grown for 24 h. Ginsenoside were dissolved and serially diluted with dimethyl sulfoxide (DMSO). Ginsenosides with various concentrations or control (0.5% of dimethyl sulfoxide) were added to cells using liquid handling station equipped with pintool system. After incubating for 2 h, glutamate (5 mM) was treated and further incubated for 16 h. Then, cells were treated with 10 μL of MTT reagent per well and incubated for 1hr. Absorbance was measured by a plate reader (Filtermax F5, Molecular Devices, San Jose, CA, USA) at 450 nm for the determination of cell viability

2.4. Live and dead assay

Cultured HT22 cells were added in 96-well black/clear bottom plates at a density 4×10^3 cells/well and grown for 24 h. The indicated concentration of Rb2 or control (0.5% of dimethyl sulfoxide) were added to 96-well plate. After incubating for 2 h, HT22 cells were treated with glutamate (5 mM) and incubated for 16 h. After incubation, cells were washed with phosphate-buffered saline (PBS) and treated with 1 μM of calcein AM and 1 $\mu\text{g}/\text{mL}$ of propidium iodide per well. Image of cells were measured using operetta high content image system (Perkin Elmer, Waltham, MA, USA)

2.5. Image analysis of 2',7'-dichlorodihydrofluorescein diacetate of HT22 cells

HT22 cells (4×10^3 cells/well) were added in 96-well black/clear bottom plates and grown at 37°C, 5% CO_2 incubator for 24 hr. The indicated concentration of Rb2 was added to 96 well plate, and 0.5% of dimethyl sulfoxide was used for control. After 2 h incubation, the HT22 cells were treated with glutamate (5 mM) and incubated for 8 h. After incubation, cells were treated with 2',7'-dichlorodihydrofluorescein diacetate (10 μM) for staining. After 30 min, PBS (50 μL , $2 \times$) was added for washing and cells were analyzed by operetta image analysis system.



- Rb1** : $\text{R}_1 = \text{Glucopyranosyl}(2\leftarrow 1)\text{Glucopyranosyl}$,
 $\text{R}_2 = \text{H}$, $\text{R}_3 = \text{Glucopyranosyl}(6\leftarrow 1)\text{Glucopyranosyl}$
Rb2 : $\text{R}_1 = \text{Glucopyranosyl}(2\leftarrow 1)\text{Glucopyranosyl}$,
 $\text{R}_2 = \text{H}$, $\text{R}_3 = \text{Glucopyranosyl}(6\leftarrow 1)\text{Arabinopyranosyl}(p)$
Rc : $\text{R}_1 = \text{Glucopyranosyl}(2\leftarrow 1)\text{Glucopyranosyl}$,
 $\text{R}_2 = \text{H}$, $\text{R}_3 = \text{Glucopyranosyl}(6\leftarrow 1)\text{Arabinofuranosyl}(f)$
Rd : $\text{R}_1 = \text{Glucopyranosyl}(2\leftarrow 1)\text{Glucopyranosyl}$, $\text{R}_2 = \text{H}$,
 $\text{R}_3 = \text{Glucopyranosyl}$
Rg1 : $\text{R}_1 = \text{H}$, $\text{R}_2 = \text{O-Glucopyranosyl}$,
 $\text{R}_3 = \text{Glucopyranosyl}(6\leftarrow 1)\text{Glucopyranosyl}$
20(S)-Rg3 : $\text{R}_1 = \text{H}$, $\text{R}_2 = \text{H}$, $\text{R}_3 = -\text{OH}$

Fig. 1. The structure of ginsenoside derivatives Rb1, Rb2, Rc, Rd, Rg1, and Rg3.

2.6. Immunoblotting analysis

60 mm dishes were used for HT22 cells (2×10^5 cells) culture. Rb2 (2.85 μM and 25.7 μM) was treated to cells and incubation continued for 16 h. Cells were homogenized in ice-cold radio-immunoprecipitation assay (RIPA) buffer (20 mM Tris-HCl, pH 7.5, 50 mM NaCl, 0.5% NP-40, 4 mM ethylenediaminetetraacetic acid (EDTA), 0.1% SDS, 0.5% sodium deoxycholate, and protease inhibitor cocktail). Protein concentrations in the lysate supernatants were measured using Bradford reagent (Bio-Rad, USA). Equal amount of protein (20 μg .) were loaded by sodium dodecyl sulfate–polyacrylamide gel electrophoresis (SDS-PAGE) and blotted onto polyvinylidene difluoride (PVDF) membranes.

Membranes were treated with primary antibodies (p38MAPK, phosphor-p38, p44/42 kinase (ERK), phospho-p44/42 (p-ERK), cleaved caspase-3, caspase-3, JNK, p-JNK, Bax, Bcl-2, GAPDH) and followed by secondary antirabbit antibodies conjugated with peroxidase (Cell Signal Technology, Boston, MA, USA). The image was acquired using chemiluminescence and analyzed with ChemiDoc XRS system (BioRad, Hercules, CA, USA).

2.7. Fluorescence cytometry analysis

HT22 cells (2×10^5 cells) cultured in 60 mm dishes were cotreated with 5 mM of glutamate and Rb2 (2.85 μM and 25.7 μM) for 16 h. Cells were harvested and treated with PI/annexin V for

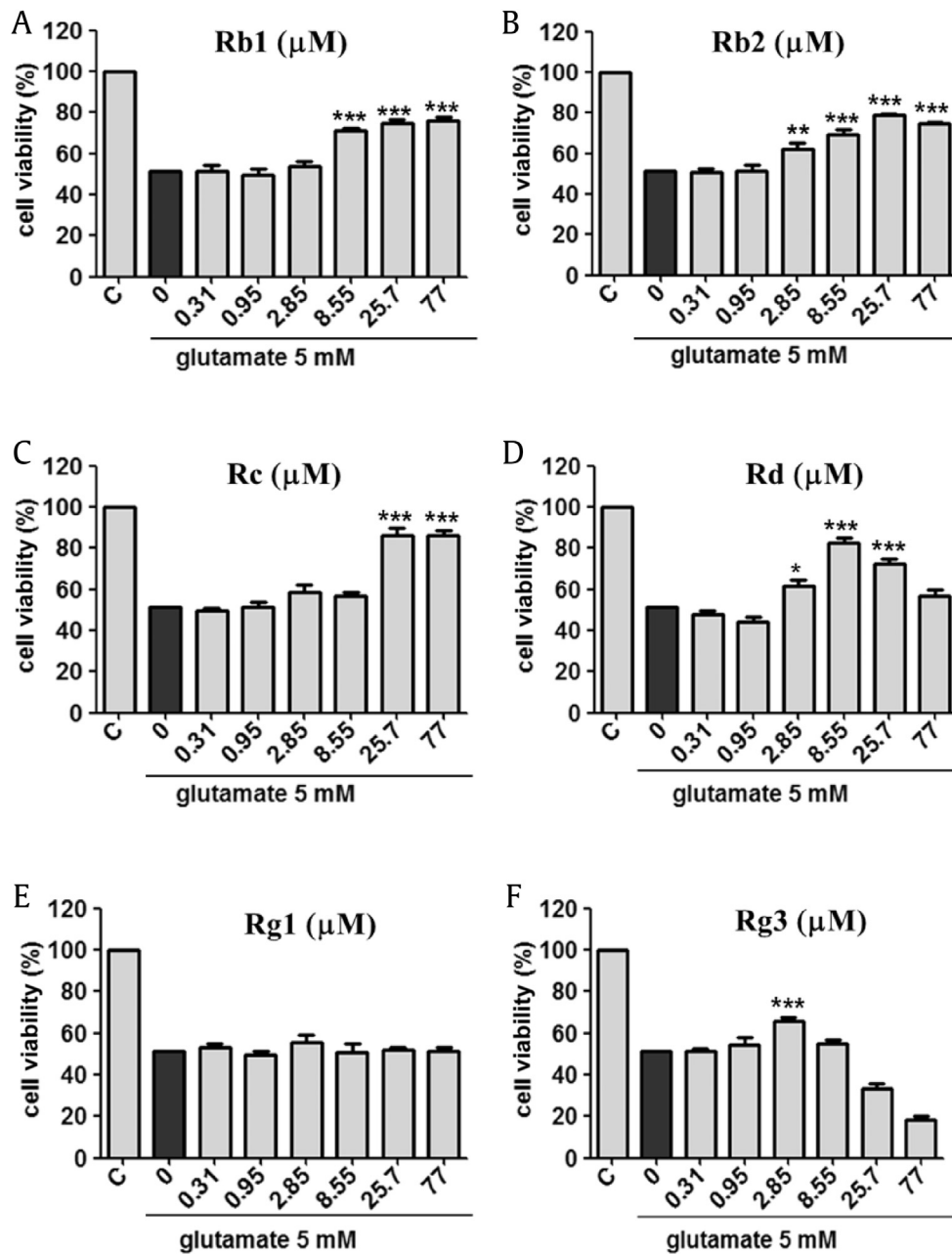


Fig. 2. The comparison of neuroprotective effects of ginsenoside derivatives ((A) Rb1, (B) Rb2, (C) Rc, (D) Rd, (E) Rg1, (F) 20(S)-Rg3) against glutamate-induced neurotoxicity in HT22 cells. 5 mM of glutamate treatment shows 50% of cell viability in HT22 cells. Ginsenoside Rb2 shows a potent neuroprotective effect against glutamate-induced cell death. *** $p < 0.001$, ** $p < 0.01$, * $p < 0.1$ compared with glutamate-treated value.

staining. Live and dead cells were determined by fluorescence cytometry (FACS) (BD Bioscience FACS Verse).

2.8. In-vivo efficacy test of ginsenoside Rb2

2.8.1. Rb2 pre-treatment

Male Mongolian gerbils (aged 6 months and 60–70g) were used for this study. The neuroprotective effect of Rb2 was examined by using a 2-VO gerbil model. The treatment protocol was permitted from the Animal Committee at Gangneung-Wonju National University. Mongolian gerbils were categorized as follows ($n = 7$, per group): (1) sham-operated gerbils (sham group), (2) vehicle-treated ischemia gerbils (vehicle group), and (3) Rb2 (10 mg/kg) treated ischemia gerbils (Rb2 group) [34]. Rb2 was mixed in vehicle (ethanol:tween 80:saline = 1:1:8). Before the surgery, vehicle or Rb2 was intraperitoneally injected (i.p.) using a 29-gauge syringe once per day for 3 days.

2.8.2. Transient cerebral ischemia induction

The Mongolian gerbils were operated after inhalation anesthesia with 2.5% isoflurane (Baxter, Deerfield, IL) in 32.2% oxygen and 65.3% nitrogen. After complete anesthesia, carotid arteries were blocked by nontraumatic aneurysm clips for 5 minutes. During the ischemic surgery, the body temperature was maintained at $37 \pm 0.5^\circ\text{C}$ using a rectal temperature probe and thermometric blanket (TR-100; Fine Science Tools, Foster City, CA). After the ischemic surgery, the Mongolian gerbils were put in the incubator until they were recovered. Sham-operated animals did not occlude

the common carotid arteries, but other procedures proceeded in the same way.

2.8.3. Histology

Four days after ischemic surgery, the Mongolian gerbils ($n = 7$, per group) were treated with sodium pentobarbital (30 mg/kg, i.p.). 0.1 M PBS (pH 7.4) followed by 4% paraformaldehyde in 0.1 M phosphate-buffer (PB, pH 7.4) was perfused transcardially into Mongolian gerbils. The brains isolated from Mongolian gerbils were quickly fixed again with 4% paraformaldehyde for 6 h. The postfixed brains infiltrated with 30% sucrose overnight for cryoprotection. These brain tissue samples were continuously cut off $30 \mu\text{m}$ thickness using a cryostat (Leica, Germany).

2.8.4. Cresyl violet staining

To confirm the survival of pyramidal cells, the brain sections were treated with cresyl violet (CV) that has high affinity to Nissle body [35]. The sections were attached to gelatin-coated slide glass and treated with 1.0% CV solution for 30 min. The stained tissues were washed with tap water and underwent a general dehydration process in serial ethanol jars. The dehydrated tissues were sealed with the permount (Sigma, USA).

2.8.5. Staining for Fluoro-Jade B

The brain tissues were stained with Fluoro-Jade B (F-J B) which has a high affinity for dead neuron [36,37]. The sections attached on the gelatin-coated slide glass were incubated in a 1% sodium hydroxide solution, 80% ethanol for 5min, and hydrated

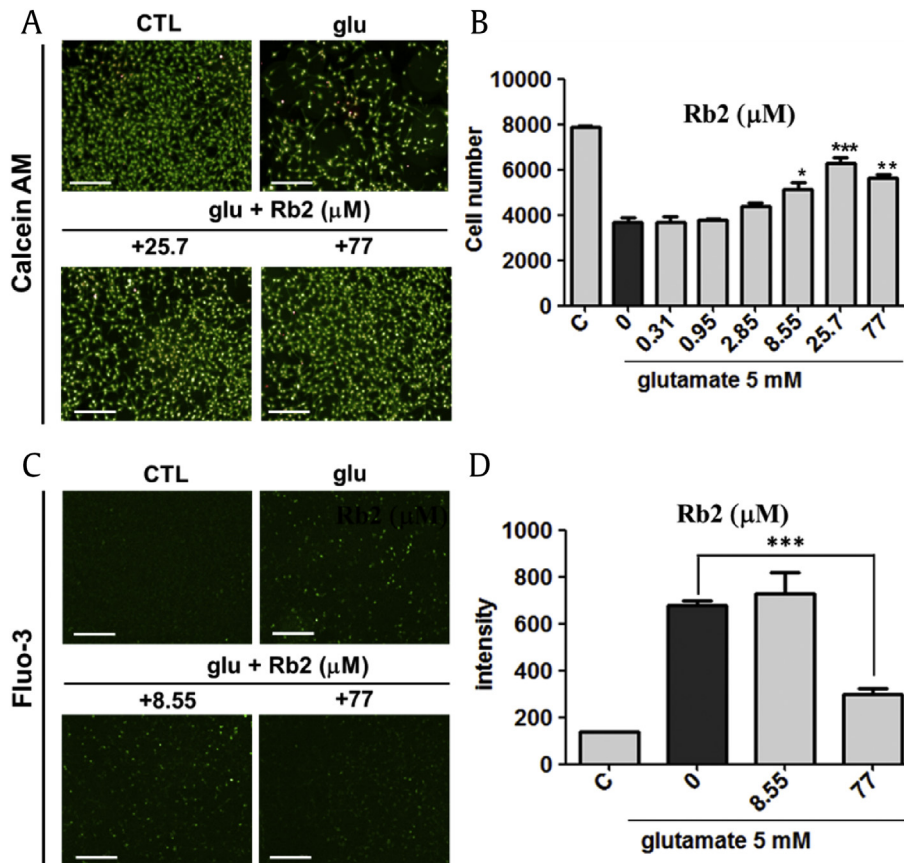


Fig. 3. (A) Live and death assay identified that ginsenoside Rb2 shows neuroprotective in glutamate-induced HT22 cell death. Calcein AM-stained live and propidium iodide-stained death cells (Scale bars = $200 \mu\text{m}$). (B) The treatment of $25.7 \mu\text{M}$ of ginsenoside Rb2 showed 80% neuroprotective effect to glutamate-induced cytotoxicity. *** $p < 0.001$, ** $p < 0.01$, * $p < 0.1$ compared with glutamate-treated value. (C) Image analysis of a fluorescent calcium sensor (Scale bars = $200 \mu\text{m}$). (D) 5 mM of glutamate treatment increased Ca^{2+} concentration in HT22 cells. $77 \mu\text{M}$ of Rb2 treatment decreased Ca^{2+} concentration in HT22 cells. *** $p < 0.05$. CTL, control.

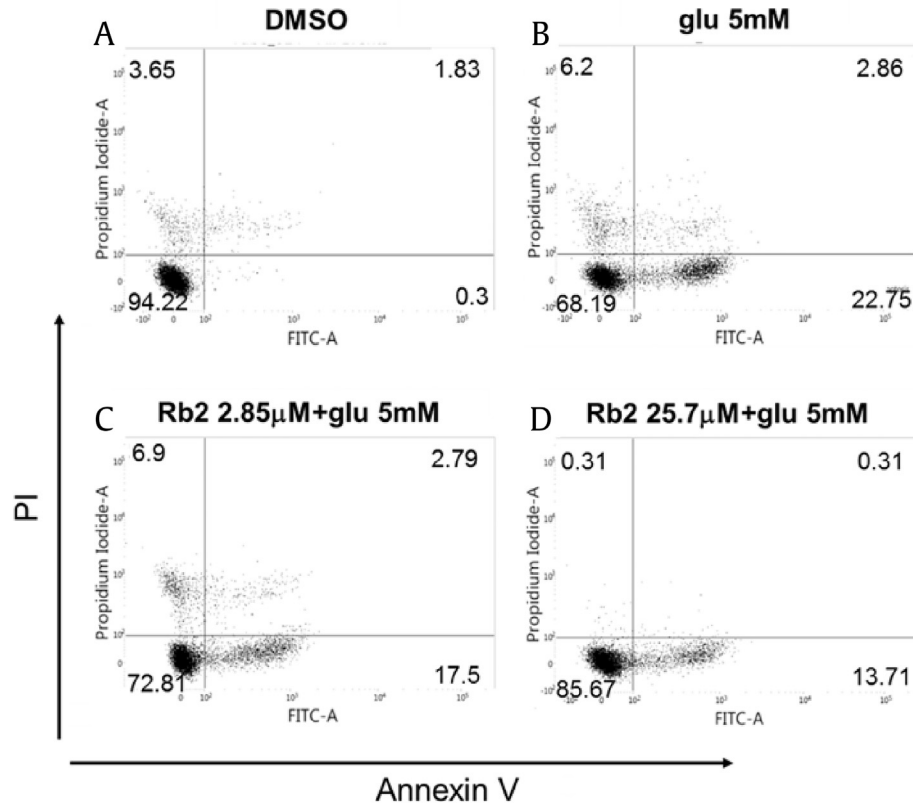


Fig. 4. Effect of ginsenoside Rb2 on glutamate-induced cell death. (A) Control. (B) The ratio of apoptotic or death cells was increased to 22.75% by the treatment of glutamate (5 mM). (C) and (D) The ratio of apoptotic or death cells was reduced to 13.71% by co-treatment of Rb2 (2.85 μ M and 25.7 μ M) and glutamate (5 mM).

in 70% ethanol-distilled water. The tissue slices were treated with a 0.06% potassium permanganate solution and shaking on a horizontal shaker for 10 min. The tissue samples were washed in distilled water and incubated in a 0.0001% F-J B (Histochem, Jefferson, AR, USA) working solution for 30 min. The stained-sections were rinsed in the distilled water and completely dried in the dry oven. The dried sections were sealed with DPX (Sigma, USA), and the image of tissue was observed by an epifluorescence microscope (AxioM1, Carl Zeiss, Göttingen, Germany) with 450–490 nm light.

2.8.6. Data analysis

Data were analyzed using the previous method [38]. Ten sections were selected at intervals of 150 μ m for quantitative analysis of CV positive or F-J B positive cells. The image of each section was captured by an AxioM1 light microscope (Carl Zeiss, Jena, Germany) attached with a digital camera (AxioCam 506, Carl Zeiss). In a 250 \times 250 μ m square at the center of striatum pyramidale in the CA1 region, CV⁺ or F-J B⁺ were counted by an image analyzing system (software: ImageJ, NIH, USA). The number of CV⁺ or F-J B⁺ cells were expressed as the average of total sections.

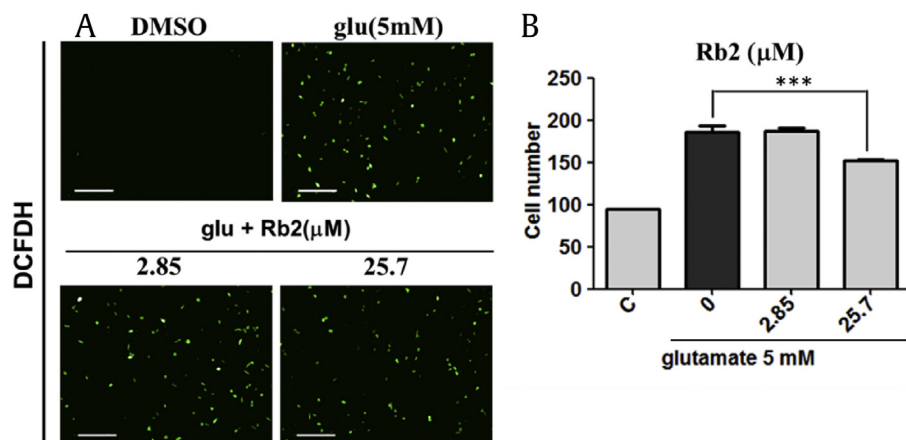


Fig. 5. Effect of ginsenoside Rb2 on glutamate-induced reactive oxygen species. (A) Visualization of calcium sensing using DCFDH. (B) Mean average of fluorescent intensity of DCF positive cells. *** p < 0.05, Scale bars = 200 μ m. DCFDH, 2',7'-dichlorodihydrofluorescein diacetate; DCF, 2',7'-dichlorodihydrofluorescein.

2.9. Statistic analysis

The Graph Pad Prism 6.0 software was used for the statistical analysis and making bar graphs. Statistical significance of the compound treatment groups was measured by one-way analysis of variance. For tissue imaging sample, statistical differences between the groups were verified by one-way analysis of variance followed by Duncan's *post hoc* test with SPSS software (SPSS, ver. 17.0, Inc., Chicago, IL, USA). The *p* values < 0.05 were used to indicate a statistical significance.

3. Result and discussion

In our study, we compared the neuroprotective capability of Rb1, Rb2, Rc, Rd, Rg1, and Rg3 (See Fig. 1) on glutamate-mediated neuronal toxicity in HT22 murine hippocampal neuronal cells. The 5 mM of glutamate has reduced the cell viability around 50% after 16 h treatment. Interestingly, the decrease in cell viability by glutamate was recovered by co-treatment with the ginsenosides. Treatment of Rc and Rd increased cell viability. However, effective concentration ranges of these ginsenoside Rc and Rd were relative narrow. Rg3 showed protective effects against glutamate-induced cell death at low concentration 2.85 μ M. High concentration of Rg3 exhibited cytotoxic effects on neuronal cells [39]. In particular, Rb1 and Rb2 exhibited the strongest protective effects in the cellular assay. Cell viability increased to more than 80% using Rb1

and Rb2 at a concentration range between 25.7 μ M and 77.0 μ M (Fig. 2). Specifically, the protective effect of Rb2 has not been previously reported; it was more pronounced than that of other ginsenosides. Using a different viability assay, HT22 cells were subjected to co-treatment with Rb2 and 5 mM of glutamate and loaded with membrane-permeable fluorescent probe calcein acetoxyethyl ester (calcein AM) to selectively stain live cells with green fluorescence (Fig. 3A). The counts of live cells were performed on images captured by fluorescence microscopy. The assay results indicated that Rb2 protected HT22 cells against glutamate-induced cytotoxicity at a concentration of 25.7 μ M. Therefore, we decided to investigate the underlying molecular mechanism associated with the Rb2-mediated neuroprotection.

To determine whether Rb2 affects glutamate-induced Ca^{2+} influx, calcium sensor Fluo-3 was monitored for the quantification of cellular Ca^{2+} concentration. The glutamate treatment increased cellular Ca^{2+} influx. After co-treatment with Rb2 and 5 mM of glutamate, the Ca^{2+} influx was reduced to half-fold (Fig. 3C and D).

As reported previously, glutamate treatment in HT22 cells shows signs of necrosis and apoptosis in a time-dependent manner [40]. So, we used PI/annexin V staining to discriminate between apoptotic and necrotic cells. After 18 h of treatment with 5 mM of glutamate, we found that cell death is associated with necrosis ($PI^{-}/annexin V^{-}$) and apoptosis ($PI^{-}/annexin V^{+}$ to $PI^{+}/annexin V^{+}$). The glutamate treatment reduced the $PI^{-}/annexin V^{-}$ stained cell population to 68.19%. In the presence of Rb2, the $PI^{-}/annexin V^{-}$

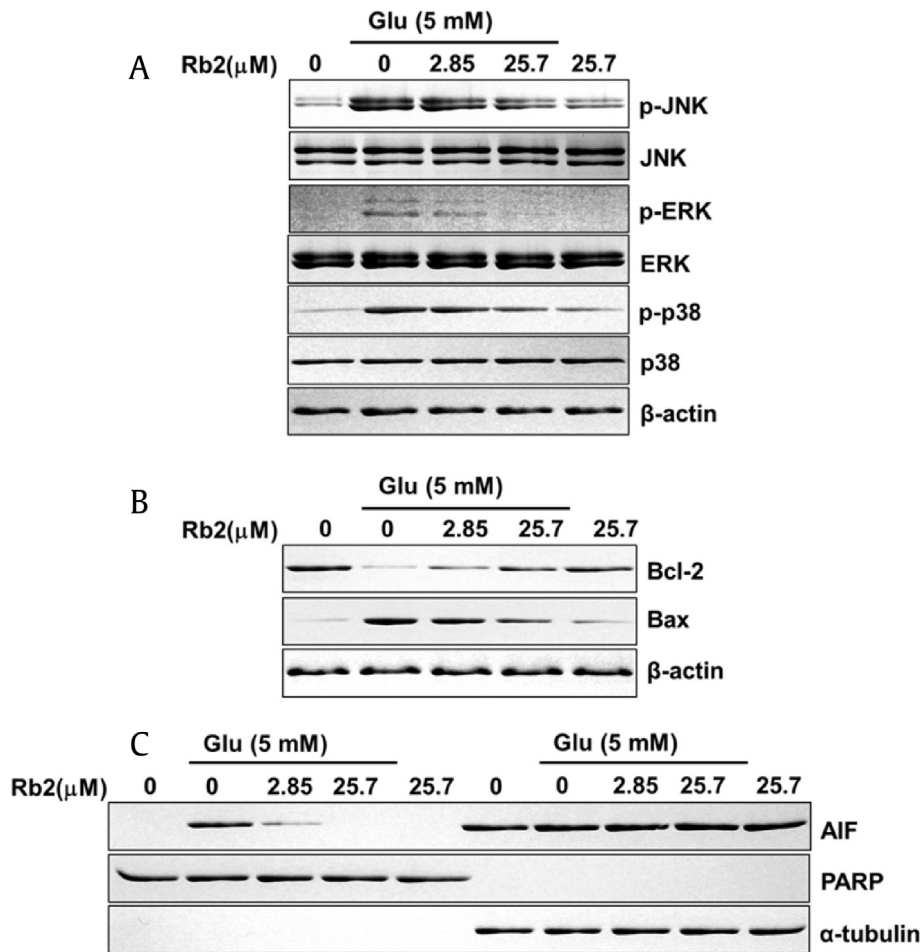


Fig. 6. Effect of ginsenoside Rb2 on MAPK, Bcl-2, Bax, and AIF expression in HT22 cells with glutamate-induced cell death. (A–C) Protein expression levels of p-JNK, JNK, p-ERK, ERK (p44/42 MAP kinase), p-p38, p38, Bcl-2, Bax, and AIF (apoptosis-inducing factor). MAPK, mitogen-activated protein kinase; ERK, extracellular signal-regulated kinase; JNK, c-Jun N-terminal kinase.

stained cell population rose to 85.0%. Thus, the FACS data indicated that Rb2 exhibited potent neuroprotective effects against glutamate treatment (Fig. 4).

We next examined whether Rb2 attenuate the glutamate-mediated intracellular ROS generation using the fluorescent reagent, 2',7'-dichlorodihydrofluorescein diacetate. The previous report showed that cellular ROS is increased in 6 h after treatment of glutamate as compared with that of untreated cells [41]. In our assay, we observed that 25.7 μ M of Rb2 prevented intracellular ROS production after 8 h of glutamate treatment (Fig. 5).

MAPKs including p38, ERK, and JNK fulfill crucial functions in apoptotic signal transduction [42]. Accumulation of intracellular ROS promotes MAPK signaling, which indicates that ROS is involved in MAPKs activation [43]. Therefore, glutamate-mediated oxidative stress cause neuronal cell death through MAPK

activation. On the contrary, treatment with chemical inhibitors (SP600125; JNK inhibitor, SB202190; p38 inhibitor or U0126; MAPK/ERK kinase inhibitor) attenuates neuronal cell death [40]. Thus, the inhibition of MAPKs activation represents a pharmacological target for neuronal cell protection. Therefore, we evaluated the effect of Rb2 on MAPKs proteins in HT22 cells. To determine the effect on the phosphorylation of MAPKs, HT22 cells were treated with 2.85 μ M and 25.7 μ M of Rb2 followed by glutamate 5 mM for 10 h. Western blot analysis showed that glutamate enhanced phosphorylation of MAPKs (ERK, JNK, and p38). However, co-treatment with Rb2 and glutamate significantly decreased MAPKs phosphorylation (Fig. 6A). Hence, we showed that Rb2 inhibited MAPKs activation, which may mediate the neuroprotection observed against glutamate-induced neurotoxicity in HT22 cells.

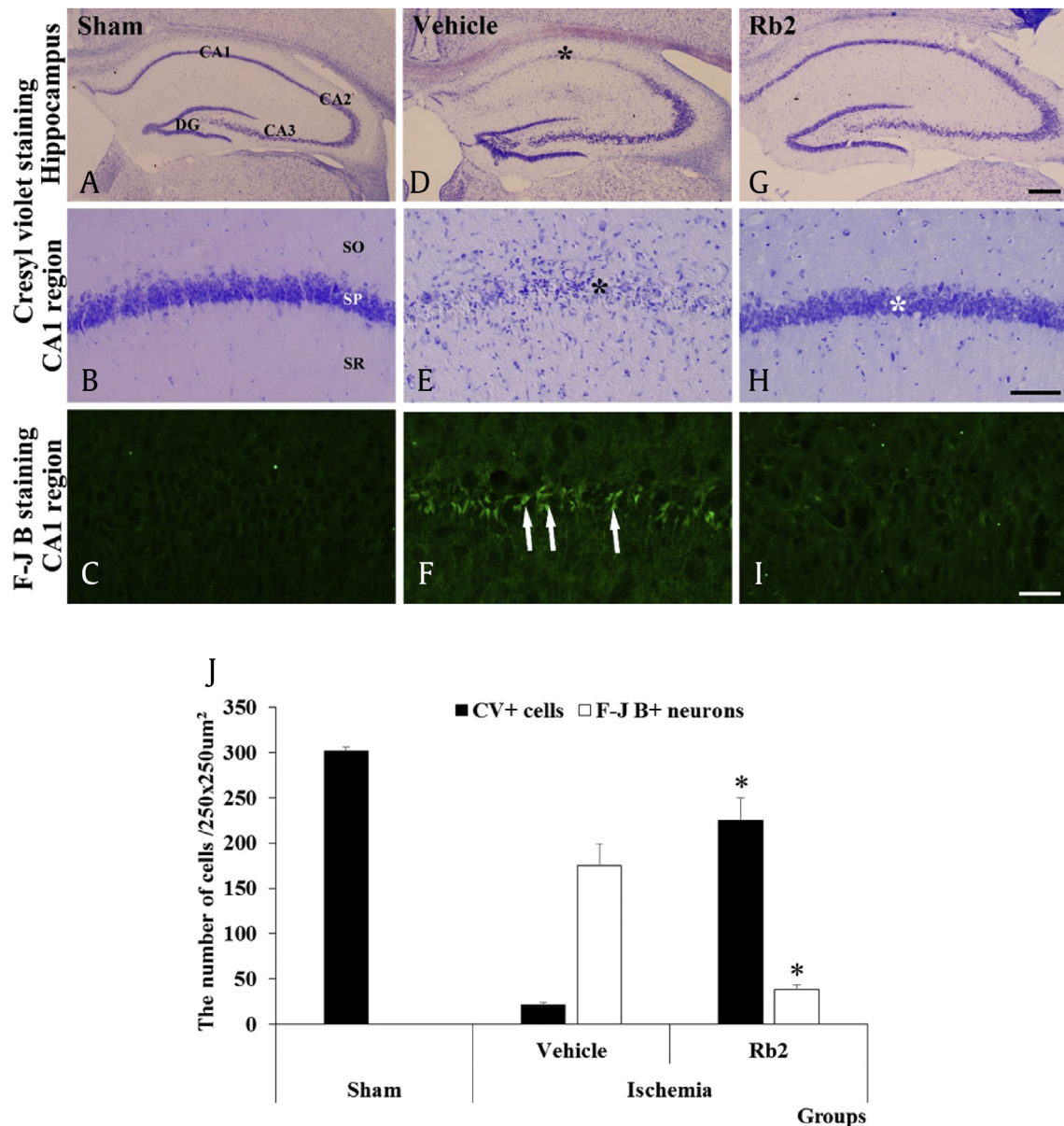


Fig. 7. CV staining (A, B, D, E, G, and F) and F-J B (C, F and I) fluorescence of the sham, vehicle and Rb2 groups 4 days after transient cerebral ischemia. CV⁺ cells in the SP of the hippocampal CA1 region (black asterisks) are hardly observed in the vehicle group (E). In the Rb group, many CV⁺ cells were detected in the SP (white asterisk). In the vehicle group, many F-J B⁺ cells (arrows) were observed in the SP; however, a few F-J B⁺ cells are detected in the Rb2 group with CV. Scale bars = 500 μ m (A, D, G), 100 μ m (B, E, H), 50 μ m (C, F, I). (J) The number of CV⁺ and F-J B⁺ cells in the hippocampal CA1 region of the sham, vehicle and Rb2 groups. ($n = 7$ per group; * $p < 0.05$, significantly different from the vehicle group). The bars indicate the means \pm SEM. (A), (D), and (G) of scale bar = 500 μ m. (B), (E), and (H) of scale bar = 100 μ m. (C), (F), and (I) of scale bar = 50 μ m. CV, cresyl violet; F-J B, Fluoro-Jade B; SP, stratum pyramidale; CA, cornu ammonis; DG, dentate gyrus; SO, stratum oriens; SR, stratum radiatum.

Bcl-2 protein family, the proapoptotic and antiapoptotic regulators are associated with glutamate mediated neuronal cell death [44,45]. Glutamate treatment alters the ratio of Bcl-2 to Bax which is a significant factor for distinguishing between proapoptotic and antiapoptotic effects [46,47]. Therefore, we studied these two protein levels in Rb2-treated samples through Western blot, and results show that the glutamate-treated cells increased the expression for proapoptotic Bax and decreased antiapoptotic Bcl-2. However, Rb2 treatment reversed the effects of glutamate (Fig. 6B).

Earlier studies reported that glutamate induces apoptosis via an AIF-dependent pathway [48,49]. Therefore, we evaluated the effect of Rb2 on the translocation of AIF to the nucleus by western blot analysis. The data have demonstrated that the glutamate treatment has increased the AIF levels in the nucleus fraction, but the Rb2 co-treatment recovered and prevented the apoptosis induction by glutamate (Fig. 6C). Our observations indicated that Rb2 inhibited accumulation of AIF into the nucleus in the presence of glutamate 5 mM. Thus, reduction of nuclear AIF by Rb2 may also contribute to the neuronal cell death-preventing effect against AIF-dependent apoptosis in HT22 cells.

We further investigated the Rb2 neuroprotection efficacy in ischemic brain injury animal model using Mongolian gerbil. In the previous report, Rb1 is known to alleviate neuronal damage induced by ischemic injury in mice [27,28], and Rg3, Rg1, and Rd function as neuroprotective agents against ischemic mouse brain injury model [49]. The Rb2 was injected into Mongolian gerbils at a daily dose of 10 mg/kg of body weight for 3 days, and then the transient cerebral ischemia was induced. The brain tissues were collected and subjected to a histopathology analysis to distinguish the normal and degenerated neurons by CV and F-J B stains, respectively (Fig. 7). CV staining data show that in the control group, most CV⁺ cells were found in the striatum pyramidal of the hippocampus region but in the ischemic damage group, it has diminished significantly. Interestingly, the Rb2 treatment group has recovered the most CV⁺ cells in the striatum pyramidal of the CA1 region in hippocampus. This data clearly shows that the Rb2 protection of pyramidal neuronal cells from ischemic damage. In F-J B staining data reveals that ischemic damage dramatically increased the number of F-J B⁺ neurons in the stratum pyramidal of the hippocampal CA1 region (Fig. 7F). However, the treatment by Rb2 decreased the number of detectable F-J B⁺ neurons which suggests that Rb2 rescues the neurons from induced cerebral ischemic damage (Fig. 7I). Our results demonstrate that the Rb2 has significant *in vivo* neuroprotective efficacy.

In this study, we have analyzed the neuroprotective effect of six ginsenosides and found that Rb2 effectively improved the viability of HT22 cells against glutamate-induced neurotoxicity. The Rb2 treatment has efficiently reduced the glutamate mediated Ca²⁺ influx and intracellular ROS accumulation. Also, Rb2 has increased the antiapoptotic Bcl-2 and decreased pro-apoptotic Bax levels. In addition, it has suppressed the MAPKs (p38, ERK, and JNK) activation caused by glutamate-mediated oxidative stress and suppressed the AIF-mediated apoptotic cell death. We identified that Rb2 increase antioxidant response element (ARE) expression which is related to protection against cellular oxidative stress (supplement figure 1S). Further, our study has showed that Rb2 has rescued the cells damaged by the ischemic brain injury and it evidently pronounces the *in vivo* neuroprotective efficacy of Rb2 in an animal model. Hence, our study suggests that, by conferring protection against glutamate-induced neuronal toxicity and ischemic brain injury, the Rb2 might have substantial therapeutic potential for various neuropathological conditions. Therefore, Rb2 may represent an interesting candidate for the development of a novel neuroprotective agent for various therapies.

We are currently performing experiments with structurally modified Rb2 derivatives to test them for improved neuroprotective effects.

Conflicts of interest

The authors have declared no conflicts of interest.

Acknowledgments

The authors thank Prof. Ki Hyun Yoo for the consorting animal study. This work was funded in part by grants from the KIST Institutional Program (2Z04690) and the National Research Council of Science & Technology (CRC-15-04-KIST).

Appendix A. Supplementary data

Supplementary data to this article can be found online at <https://doi.org/10.1016/j.jgr.2018.12.002>.

References

- [1] Riedel G, Platt P, Micheau J. Glutamate receptor function in learning and memory. *Behav Brain Res* 2003;140:1–47.
- [2] Reynolds IJ, Hastings TG. Glutamate induces the production of reactive oxygen species in cultured forebrain neurons following NMDA receptor activation. *J Neurosci* 1995;15:3318–27.
- [3] Choi DW. Glutamate neurotoxicity and diseases of the nervous system. *Neuron* 1988;1:623–34.
- [4] Dong XX, Wang Y, Qin ZH. Molecular mechanisms of excitotoxicity and their relevance to pathogenesis of neurodegenerative diseases. *Acta Pharmacol Sin* 2009;30:379–87.
- [5] Coyle TJ, Puttfarcken P. Oxidative stress, glutamate, and neurodegenerative disorders. *Science* 1993;262:689–95.
- [6] Niikura T, Tajima H, Kita Y. *Curr Neuropharmacol* 2006;4:139–47.
- [7] Cookson MR. *Mol Neurodegener* 2009;4:9.
- [8] Cowan CM, Raymond LA. *Curr Top Dev Biol* 2006;75:25–71.
- [9] Murphy TH, Miyamoto M, Sastre A, Schnaar RL, Coyle JT. Glutamate toxicity in a neuronal cell line involves inhibition of cysteine transport leading to oxidative stress. *Neuron* 1989;2:1547–58.
- [10] Choi DW. Glutamate neurotoxicity and diseases of the nervous system. *Neuron* 1988;1:623–34.
- [11] Tan S, Schubert D, Maher P. Oxytosis: a novel form of programmed cell death. *Curr Top Med Chem* 2001;1:497–506.
- [12] Kang Y, Tiziani S, Park G, Kaul M, Paternostro G. Cellular protection using Flt3 and PI3K α inhibitors demonstrates multiple mechanisms of oxidative glutamate toxicity. *Nat Comm* 2014;5:1–12.
- [13] Yang E-J, Song K-S. Polyozellin, a key constituent of the edible mushroom *Polyozellus multiplex*, attenuates glutamate-induced mouse hippocampal neuronal HT22 cell death. *Food Funct* 2015;6:3678–86.
- [14] Tobaben S, Grohm J, Seiler A, Conrad M, Plesnila N, Culmsee C. Bid-mediated mitochondrial damage is a key mechanism in glutamate-induced oxidative stress and AIF-dependent cell death in immortalized HT-22 hippocampal neurons. *Cell Death Differ* 2011;18:282–92.
- [15] Culmsee C, Plesnila N. Targeting Bid to prevent programmed cell death in neurons. *Biochem Soc Trans* 2006;34:1334–40.
- [16] Xu X, Chua CC, Kong J, Kostrzewa RM, Kumaraguru U, Hamdy RC, Chua BH. Necrostatin-1 protects against glutamate-induced glutathione depletion and caspase-independent cell death in HT-22 cells. *J Neurochem* 2007;103:2004–14.
- [17] Landshamer S, Hoehn M, Barth N, Duvezin-Caubet S, Schwake G, Tobaben S, Kazhdan I, Becattini B, Zahler S, Vollmar A, et al. Bid-induced release of AIF from mitochondria causes immediate neuronal cell death. *Cell Death Differ* 2008;15:1553–63.
- [18] Susin SA1, Lorenzo HK, Zamzami N, Marzo I, Snow BE, Brothers GM, Mangion J, Jacotot E, Costantini P, Loeffler M, et al. Molecular characterization of mitochondrial apoptosis-inducing factor. *Nature* 1999;397:441–6.
- [19] Daugas EI, Susin SA, Zamzami N, Ferri KF, Irinopoulou T, Larochette N, Prévost MC, Leber B, Andrews D, Penninger J, et al. Mitochondrio-nuclear translocation of AIF in apoptosis and necrosis. *FASEB J* 2000;14:729–39.
- [20] Ray PD, Huang BW, Tsuji Y. Reactive oxygen species (ROS) homeostasis and redox regulation in cellular signaling. *Cell Signal* 2012;24:981–90.
- [21] Choi JH, Choi AY, Yoon H, Choe W, Yoon K-S, Ha J, Yeo E-J, Kang I. Baicalein protects HT22 murine hippocampal neuronal cells against endoplasmic reticulum stress-induced apoptosis through inhibition of reactive oxygen species production and CHOP induction. *Exp Mol Med* 2010;42:811–22.

- [22] Pearson G, Robinson F, Beers Gibson T, Xu BE, Karandikar M, Berman K, Cobb MH. Mitogen-activated protein (MAP) kinase pathways: regulation and physiological functions. *Endocr Rev* 2001;22:153–83.
- [23] Tibbles LA, Woodgett JR. The stress-activated protein kinase pathways. *Cell Mol Lif Sci* 1999;55:1230–54.
- [24] Park EH, Kim YJ, Yamabe N, Park SH, Kim HK, Jang HJ, Kim JH, Cheon GJ, Ham J, Kang KS. Stereospecific anticancer effects of ginsenoside Rg3 epimers isolated from heat-processed American ginseng on human gastric cancer cell. *J Ginseng Res* 2014;38:22–7.
- [25] Park JY, Choi P, Kim HK, Kang KS, Ham J. Increase in apoptotic effect of Panax ginseng by microwave processing in human prostate cancer cells: in vitro and in vivo studies. *J Ginseng Res* 2016;40:62–7.
- [26] Jang HJ, Han IH, Kim YJ, Yamabe N, Lee D, Hwang GS, Oh M, Choi KC, Kim SN, Ham J, et al. Anticarcinogenic effects of products of heat-processed ginsenoside Re, a major constituent of ginseng berry, on human gastric cancer cells. *J Agric Food Chem* 2014;62:2830–6.
- [27] Dong X, Zheng L, Lu S, Yang Y. Neuroprotective effects of pretreatment of ginsenoside Rb1 on severe cerebral ischemia-induced injuries in aged mice: involvement of anti-oxidant signaling. *Geriatr Gerontol Int* 2017;17:338–45.
- [28] Gao XQ, Yang CX, Chen GJ, Wang GY, Chen B, Tan SK, Liu J, Yuan QL. Ginsenoside Rb1 regulates the expressions of brain-derived neurotrophic factor and caspase-3 and induces neurogenesis in rats with experimental cerebral ischemia. *J Ethnopharmacol* 2010;132:393–9.
- [29] Wang L, Zhao H, Zhai ZZ, Qu LX. Protective effect and mechanism of ginsenoside Rg1 in cerebral ischaemia-reperfusion injury in mice. *Biomed Pharmacother* 2018;99:876–82.
- [30] Zhang G, Xia F, Zhang Y, Zhang X, Cao Y, Wang L, Liu X, Zhao G, Shi M. Ginsenoside Rd is efficacious against acute ischemic stroke by suppressing microglial proteasome-mediated inflammation. *Mol Neurobiol* 2016;53:2529–40.
- [31] Kim JH, Cho SY, Lee JH, Jeong SM, Yoon IS, Lee BH, Lee JH, Pyo MK, Lee SM, Chung JM, et al. Neuroprotective effects of ginsenoside Rg3 against homocysteine-induced excitotoxicity in rat hippocampus. *Brain Res* 2007;1136:190–9.
- [32] Tian J, Fu F, Geng M, Jiang Y, Yang J, Jiang W, Wang C, Liu K. Neuroprotective effect of 20(S)-ginsenoside Rg3 on cerebral ischemia in rats. *Neurosci Lett* 2005;374:92–7.
- [33] Tan S, Wood M, Maher P. Oxidative stress induces a form of programmed cell death with characteristics of both apoptosis and necrosis in neuronal cells. *J Neurochem* 1998;71:95–105.
- [34] Wen T-C, Yoshimura H, Matsuda S, Lim J-H, Sakanaka M. Ginseng root prevents learning disability and neuronal loss in gerbils with 5-minute forebrain ischemia. *Acta Neuropathol* 1996;91:15–22.
- [35] Lee JC, Park JH, Ahn JH, Kim IH, Cho JH, Choi JH, Yoo KY, Lee CH, Hwang IK, Cho JH, et al. New GABAergic neurogenesis in the hippocampal CA1 region of a gerbil model of long-term survival after transient cerebral ischemic injury. *Brain Pathol* 2016;26:581–92.
- [36] Schmued LC, Hopkins KJ, Fluoro-Jade B. A high affinity fluorescent marker for the localization of neuronal degeneration. *Brain Res* 2000;874:123–30.
- [37] Park JH, Joo HS, Yoo KY, Shin BN, Kim IH, Lee CH, Choi JH, Byun K, Lee B, Lim SS, et al. Extract from Terminalia chebula seeds protect against experimental ischemic neuronal damage via maintaining SODs and BDNF levels. *Neurochem Res* 2011;36:2043–50.
- [38] Park JH, Shin BN, Chen BH, Kim IH, Ahn JH, Cho JH, Tae HJ, Lee JC, Lee CH, Kim YM, et al. Neuroprotection and reduced gliosis by atomoxetine pretreatment in a gerbil model of transient cerebral ischemia. *J Neurol Sci* 2015;359:373–80.
- [39] Kim YC, Kim SR, Markelonis GJ, Oh TH. Ginsenosides Rb1 and Rg3 protect cultured rat cortical cells from glutamate-induced neurodegeneration. *J Neurosci Res* 1998;53:426–32.
- [40] Fukui M, Song JM, Choi JY, Choi HJ, Zhu BT. Mechanism of glutamate-induced neurotoxicity in TH22 mouse hippocampal cells. *Euro J of Pharm* 2009;617:1–11.
- [41] Son Y, Cheong YK, Kim NH, Chung HT, Kang DG, Pae HO. Mitogen-activated protein kinases and reactive oxygen species; how can ROS activate MAPK pathways? *J Signal Transduct* 2011;2011:792639.
- [42] Ray PD, Huang BW, Tsuji Y. Reactive oxygen species (ROS) homeostasis and redox regulation in cellular signaling. *Cell Signaling* 2012;24:981–90.
- [43] Pettmann B1, Henderson CE. Neuronal cell death. *Neuron* 1998;20:633–47.
- [44] Bredesen DE. Neural apoptosis. *Ann Neurol* 1995;38:839–51.
- [45] Zhang Y, Lu X, Bhavnani BR. Equine estrogens differentially inhibit DNA fragmentation induced by glutamate in neuronal cells by modulation of regulatory proteins involved in programmed cell death. *BMC Neurosci* 2003;4:32.
- [46] Yang E-J, Min JS, Ku H-Y, Choi H-S, Park M, Kim MK, Song K-S, Lee D-S. Isoliquiritigenin isolated from *Glycyrrhiza uralensis* protects neuronal cells against glutamate-induced mitochondrial dysfunction. *Biochem Biophys Res Comm* 2012;421:658–64.
- [47] Landshamer S, Hoehn M, Barth N, Duvezin-Caubet S, Schwake G, Tobaben S, Kazhdan I, Becattini B, Zahler S, Vollmar A, et al. Bid-induced release of AIF from mitochondria causes immediate neuronal cell death. *Cell Death Diff* 2008;15:1553–63.
- [48] Tobaben S, Grohm J, Seiler A, Conrad M, Plesnila N, Culmsee C. Bid-mediated mitochondrial damage is a key mechanism in glutamate-induced oxidative stress and AIF-dependent cell death in immortalized HT-22 hippocampal neurons. *Cell Death Diff* 2011;18:282–92.
- [49] Ong W-Y, Farooqui T, Koh H-L, Farooqui AA, Ling E-A. Protective effects of ginseng on neurological disorders. *Front Aging Neurosci* 2015;7:129.